Regioselectivity of Phase II Metabolism of Luteolin and Quercetin by UDP-Glucuronosyl Transferases

ARTICLE *in* CHEMICAL RESEARCH IN TOXICOLOGY · JUNE 2002

Impact Factor: 3.53 · DOI: 10.1021/tx0101705 · Source: PubMed

9 AUTHORS, INCLUDING:

Sjef Boeren
Wageningen University
124 PUBLICATIONS **3,881** CITATIONS
SEE PROFILE

J.J.M. Vervoort
Wageningen University
397 PUBLICATIONS **7,795** CITATIONS
SEE PROFILE

Nicole H P Cnubben
TNO
69 PUBLICATIONS **2,351** CITATIONS
SEE PROFILE

Peter J van Bladeren
Nestlé S.A.
428 PUBLICATIONS **10,366** CITATIONS
SEE PROFILE

Regioselectivity of Phase II Metabolism of Luteolin and Quercetin by UDP-Glucuronosyl Transferases

Marelle G. Boersma,[†,‡] Hester van der Woude,[†] Jan Bogaards,[§] Sjef Boeren,[‡] Jacques Vervoort,[‡] Nicole H. P. Cnubben,[§,||] Marlou L. P. S. van Iersel,[⊥] Peter J. van Bladeren,[†,§,||] and Ivonne M. C. M. Rietjens*[,†,||]

Division of Toxicology, Wageningen University, Tuinlaan 5, 6703 HE, Wageningen, The Netherlands, Laboratory of Biochemistry, Wageningen University, Dreijenlaan 3, 6703 HA, Wageningen, The Netherlands, TNO Nutrition and Food Research, P.O. Box 360, 3700 AJ, Zeist, The Netherlands, WU/TNO Centre for Food Toxicology, P.O. Box 8000, 6700 EA, Wageningen, The Netherlands, and N.V. Organon, P.O. Box 20, 5340 BH, Oss, The Netherlands

Received November 2, 2001

The regioselectivity of phase II conjugation of flavonoids is expected to be of importance for their biological activity. In the present study, the regioselectivity of phase II biotransformation of the model flavonoids luteolin and quercetin by UDP-glucuronosyltransferases was investigated. Identification of the metabolites formed in microsomal incubations with luteolin or quercetin was done using HPLC, LC-MS, and ^{1}H NMR. The results obtained demonstrate the major sites for glucuronidation to be the 7-, 3-, 3′-, or 4′-hydroxyl moiety. Using these unequivocal identifications, the regioselectivity of the glucuronidation of luteolin and quercetin by microsomal samples from different origin, i.e., rat and human intestine and liver, as well as by various individual human UDP-glucuronosyltransferase isoenzymes was characterized. The results obtained reveal that regioselectivity is dependent on the model flavonoid of interest, glucuronidation of luteolin and quercetin not following the same pattern, depending on the isoenzyme of UDP-glucuronosyltransferases (UGT) involved. Human UGT1A1, UGT1A8, and UGT1A9 were shown to be especially active in conjugation of both flavonoids, whereas UGT1A4 and UGT1A10 and the isoenzymes from the UGTB family, UGT2B7 and UGT2B15, were less efficient. Due to the different regioselectivity and activity displayed by the various UDP-glucuronosyltransferases, regioselectivity and rate of flavonoid conjugation varies with species and organ. Qualitative comparison of the regioselectivities of glucuronidation obtained with human intestine and liver microsomes to those obtained with human UGT isoenzymes indicates that, in human liver, especially UGT1A9 and, in intestine, UGT1A1 and UGT1A8 are involved in glucuronidation of quercetin and luteolin. Taking into account the fact that the anti-oxidant action as well as the pro-oxidant toxicity of these catechol-type flavonoids is especially related to their 3′,4′-dihydroxyl moiety, it is of interest to note that the human intestine UGT's appear to be especially effective in conjugating this 3′,4′ catechol unit. This would imply that upon glucuronidation along the transport across the intestinal border, the flavonoids loose a significant part of these biological activities.

Introduction

Luteolin and quercetin (Figure 1) are important members of the class of flavonoid food components. These flavonoids are polyphenols, which are important constituents of fruit, vegetables, red wine, and tea. The antioxidant properties of flavonoids are often claimed to be responsible for the protective effects of these compounds against cardiovascular disease, certain forms of cancer, and/or photosensitivity diseases (*1*−*4*). Because of these beneficial health claims, the interest for the use of flavonoids such as quercetin and luteolin as functional food ingredients is increasing rapidly. However, other research data point at possible toxic pro-oxidant action of flavonoids. This includes the formation of reactive mutagenic quinoid-type metabolites from especially 3′,4′-dihydroxy (= catechol)-type polyphenol antioxidants such as the flavonoid quercetin (*1*, *5*−*8*). The anti- as well as the pro-oxidant effects of flavonoids have been reported to be highly dependent on the number and position of the hydroxyl moieties in the flavonoid molecule. To achieve an efficient antioxidant action, several studies

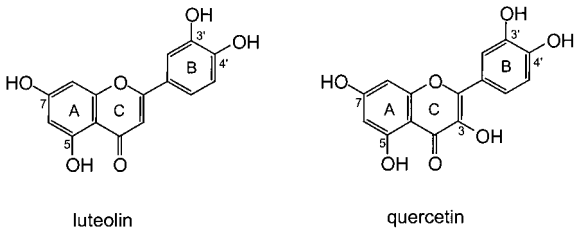

Figure 1. Chemical structures of luteolin and quercetin.

* To whom correspondence should be addressed. Fax: (31) (317) 484801. E-mail: ivonne.rietjens@algemeen.tox.wau.nl.
† Division of Toxicology, Wageningen University.
‡ Laboratory of Biochemistry, Wageningen University.
§ TNO Nutrition and Food Research.
|| TNO Centre for Food Toxicology.
⊥ N.V. Organon.

10.1021/tx0101705 CCC: $22.00
Published on Web 04/19/2002

have reported the importance of a 3′,4′-dihydroxy moiety in the B-ring, the 2,3-double bond in combination with a 4-oxo function in the C ring and the additional presence of 3- and 5-hydroxyl groups in the flavonoid molecular structure (*2*, *9*). Data on pro-oxidant activities indicate similar structural features to be essential for mutagenic and other pro-oxidant activities (*5*, *8*, *10*, *11*).

Since the hydroxyl substituent pattern significantly affects the anti- as well as the pro-oxidant biological activity of the flavonoids, the regioselectivity of their conjugation can be expected to influence these biological activities as well. Naturally occurring flavonoids are often glycosylated or glucuronidated, but may become deconjugated by bacterial activity in the gut and/or during transport over the gut wall (*12*). Upon and/or during absorption, biotransformation of the flavonoids (methylation, glucuronidation, and sulfation) may result in conjugated metabolites with different properties, depending on the position at which conjugation occurs. Cao et al. (*13*) concluded that the more hydroxyl substituents, the stronger the antioxidant but also the pro-oxidant activity of flavonoids and that O-methylation of the hydroxyl groups inactivates both these activities of flavonoids. Glucuronidation of the 3′- or 4′-hydroxyl group in the B-ring of flavonoids would increase the reduction potential and therefore decrease the antioxidant activity, whereas glucuronidation in the A-ring would affect antioxidant activity to a lesser extent (*14*). With respect to the influence of conjugation on toxic effects, it has been reported that O-methylation of the 3′,4′-catechol moiety results in detoxification of quercetin and fisetin (*15*). Although the metabolism of flavonoids is a growing field of interest (*15*−*21*), much about the uptake and metabolism of dietary flavonoids remains unknown (*22*). This holds especially for knowledge on the regioselectivity of flavonoid conjugation.

Therefore, the objective of the present study was to identify the major sites for glucuronidation of two model flavonoids, luteolin and quercetin (Figure 1). Luteolin is a member of the flavone subclass of flavonoids and usually occurs as a glycosylated form in celery, perilla leaves, green pepper, and camomile tea and as aglycone in perilla seeds and in parsley (*23*). Recently, several groups have reported intestinal absorption and metabolism of luteolin in rats and humans (*12*, *20*, *24*), but these studies did not identify the exact nature and regioselectivity of the metabolites formed. Quercetin glycosides represent the predominant flavonoid fraction present in fruits and vegetables, especially onions, broccoli, and apples (*22*, *25*) as well as in tea and red wine. Several studies report glucuronidated, sulfated, and/or methylated quercetin metabolites in plasma of man and rats upon quercetin exposure (*18*, *19*, *21*, *26*−*28*), but again the exact regioselectivity of the conjugate formation was not elucidated. Recently Day et al. (*29*) reported HPLC UV-vis based identification of quercetin glucuronosyls formed by human liver cell free extracts showing conjugation at 4′-, 3′-, 7-, and 3-OH, the highest rate of conversion being observed for the 3′-position. In the present study, the regioselectivity of quercetin but also luteolin conjugation was investigated using LC-MS and especially ^{1}H NMR as the method of choice for identification of the conjugates. In addition, the present study reports on the regioselectivity of glucuronidation of the two model flavonoids by individual UDP-glucuronosyltransferase isoenzymes.

Experimental Procedures

Materials. Quercetin was obtained from Acros Organics (New Jersey). Isoquercetrin, luteolin, luteolin-7-glucoside, and luteolin-4′-glucoside were purchased from Indofine (Somerville, PA). All flavonoid substrates were prepared fresh as a stock solution in DMSO or DMSO-d_6 in the case of ^{1}H NMR measurements. 4-Trifluoromethyl-7-hydroxycoumarin was purchased from Enzyme Systems Products (Dublin, CA). Alamethicin, uridine 5′-diphosphoglucuronic acid (UDPGA), and trifluoperazine were obtained from Sigma (St. Louis, MO). β-Glucuronidase was from Boehringer (Mannheim, Germany). DMSO-d_6 and D_2O were obtained from ARC Laboratories (Amsterdam, The Netherlands). Trifluoroacetic acid was obtained from Merck (Darmstadt, Germany). Acetonitril was HPLC grade and purchased from Lab-Scan Ltd. (Dublin, Ireland).

Rat liver microsomes were prepared from perfused livers from Wistar rats as described before (*30*) and human liver microsomes were prepared from human liver samples as described previously (*31*). Human intestine microsomes (pooled from 10 healthy individuals) were obtained from In Vitro Technologies (Baltimore, MD) and microsomes from rat intestine from Biopredic International (Rennes, France). Microsomes (UGT1A6 and UGT1A9) and Supersomes (UGT1A1, UGT1A3, UGT1A4, UGT1A8, UGT1A10, UGT2B7, and UGT2B15) from cell lines transfected with cDNAs expressing human UGTs were obtained from GENTEST Corp. (Woburn, MA).

Liver and Intestine Microsomal Incubations. Incubation mixtures contained 0.1 M potassium phosphate, pH 7.4, 0.5 or 2 mg/mL microsomal protein (as indicated), 100 μM luteolin or quercetin, added as a 100 times concentrated stock solution in DMSO. The reaction was started by adding 4 mM (final concentration) UDPGA and incubated at 37 °C for 15 min. Samples were either frozen in liquid nitrogen before analysis or analyzed directly by HPLC.

Quantification of the glucuronosyl metabolites formed by microsomal incubations was done on the basis of the peak area in the HPLC chromatogram at 345 nm for luteolin and 370 nm for quercetin, assuming similar ϵ value of flavonoids and their glucuronosyl conjugates (*22*). The UV−vis absorption spectra reveal this to be a reasonable assumption because the effects of conjugation on the UV−vis spectra are not significant.

Incubations with Individual UGT-Isoenzymes. Incubation mixtures contained 0.1 M Tris-HCl pH 7.5, 1 mM DTT, 10 mM $MgCl_2$, 25 μg/mL alamethicin, 0.5 mg/mL microsomal protein, 100 μM luteolin or quercetin, added as a 100 times concentrated stock solution in DMSO and 1 mM UDPGA and were incubated for 30 min at 37 °C. The reaction was stopped by adding 100 μL of acetonitril:acetic acid (94:6) (v/v) to 200 μL incubation mixture. After centrifugation (5 min at 2750*g*), the samples were stored at − 20 °C until analyzed by HPLC.

Activities of the commercially obtained UGT1A1, UGT1A3, UGT1A6, UGT1A8, UGT1A9, UGT1A10, UGT2B7, and UGT2B15 isoenzyme preparations were checked on the basis of activity toward the standard substrate 4-trifluoromethyl-7-hydroxycoumarin and were as follows: 795, 730, 7430, 350, 2300, 90, 1510, and 1860 pmol/min/mg of protein, respectively. The enzyme activity of UGT1A4 toward trifluoperazine was 1070 pmol/min/mg of protein. These assays were described by the supplier using standard methods (GENTEST Corp.) and the activities were in line with literature data and validate the quality of the UGT enzyme preparations used.

Enzymatic Deconjugation. To confirm the nature of the glucuronosyl conjugates, medium samples were treated with β-glucuronidase. To this end, 10 μL of sample was added to 90 μL of 200 mM potassium phosphate, pH 6.2 and after addition of 3 μL of β-glucuronidase solution (0.8 units) the mixture was incubated for 1 h at 37 °C. After the incubation, the mixtures were either frozen in liquid nitrogen before analysis or analyzed directly by HPLC.

HPLC Analysis. HPLC was performed with a Waters M600 liquid chromatography system. Reaction product analysis was achieved using an Alltima C18 5U column (4.6 × 150 mm;

Alltech, Breda, The Netherlands), eluted at a flow of 1 mL/min with a gradient starting at 17% acetonitril in Nanopure water containing 0.1% trifluoroacetic acid for 2 min, followed by a gradient of 17% to 25% acetonitril in 5 min, increasing to 35% in 8 min, to 50% in 5 min and increasing to 100% acetonitril in 5 min, finally keeping this percentage for 2 min, followed by a reequilibration at 17% acetonitril in Nanopure water containing 0.1% trifluoroacetic acid for 10 min.

In a typical run, aliquots of 10 μL of the incubation mixture were injected. Detection was performed between 230 and 420 nm using a Waters 996 photodiode array detector. Chromatograms presented are based on detection at 345 nm for luteolin and 370 nm for quercetin incubations.

To collect the different metabolites for product identification, similar HPLC runs were performed except for the fact that luteolin or quercetin were added at least three times to the incubation mixtures followed by 10 min incubation at 37 °C, before injecting 50 μL of the incubation mixture onto the HPLC column. Product peaks of successive runs were collected, pooled, freeze-dried and dissolved in DMSO-d_6 for ^{1}H NMR analysis.

LC-MS Analysis. Incubation samples were analyzed by LC-MS. Mass spectrometric analysis (Finnigan MAT 95, San Jose, CA) was performed in the negative electrospray mode using a spray voltage of 4.5 kV and a capillary temperature of 180 °C with nitrogen as sheath and auxiliary gas. For LC, the same conditions as described above were used, except that in eluent A 0.1% trifluoroacetic acid was replaced by 0.1% acetic acid, which had no effect on retention times.

^{1}H NMR Analysis. The glucuronosyl conjugates were characterized by ^{1}H NMR using a Bruker DPX 400 MHz or a Bruker AMX 500 MHz spectrometer. A 1.5 s presaturation delay was used, a 60° pulse angle and a 2.2 s acquisition time (7575 Hz sweep width, 32 K data points). The data were processed using an exponential multiplication of 0.5 or 1.0 Hz and zero filling to 64 K data points. Resonances are reported relative to DMSO at 2.50 ppm.

Results

Identification of Luteolin Glucuronosyls. Figure 2a shows a typical HPLC chromatogram of an incubation of 100 μM luteolin with rat liver microsomes. The chromatogram shows that with rat liver microsomes, upon 15 min of incubation with UDPGA, three metabolites, with retention times at 11.4 ± 0.2, 13.9 ± 0.2, and 14.5 ± 0.2 min, are formed. HPLC analysis of the incubations of luteolin with human liver microsomes (Figure 2c) reveals formation of the same three metabolites only at a different ratio (Table 1). Figure 2, panels b and d, presents the HPLC chromatograms of similar incubations using rat and human intestine microsomes. The same three metabolites are formed at again a different ratio (Table 1). Comparison of these ratios reveals that regioselectivity of the glucuronidation varies between organs as well as between species (Table 1). Increasing the concentration of microsomal protein in the incubations from 0.5 to 2 mg/mL increased the overall conversion upon 15 min incubation 2.5 times but did not affect the regioselectivity, i.e., the ratio between the different conjugates formed.

Incubation of the samples with β-glucuronidase results in complete elimination of the three metabolite peaks and a concomitant increase of the luteolin peak (HPLC chromatograms not shown), indicating that all metabolite peaks represent glucuronidated luteolin derivatives.

To identify the exact nature of the glucuronosyl conjugates, samples from the microsomal incubations were also analyzed by LC-MS. The results obtained reveal for the three metabolites a *m*/*z* value of 461 representing the [M − H]-mass of a luteolin monoglucuronosyl.

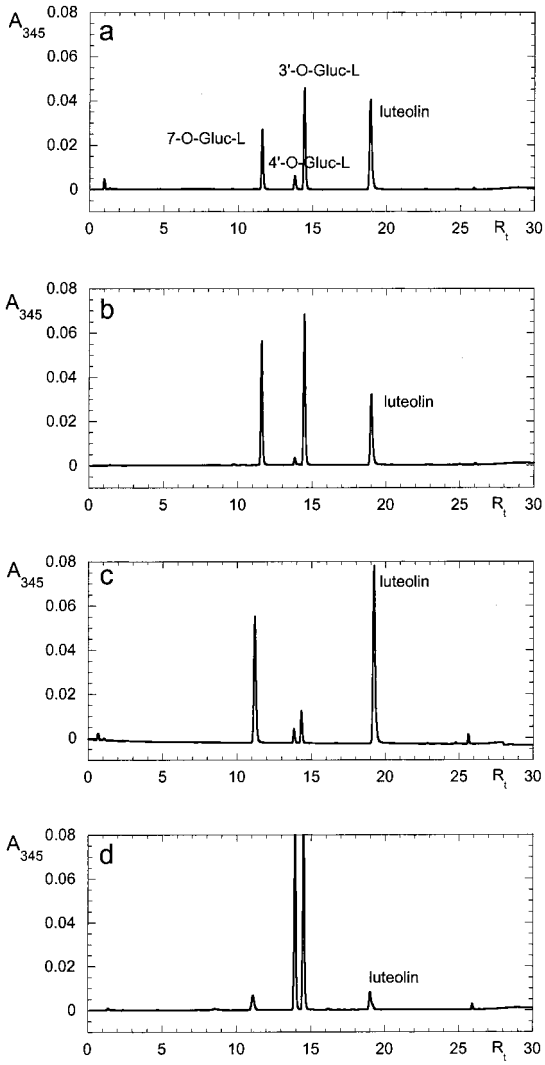

Figure 2. HPLC chromatogram of incubations of luteolin with (a) rat liver microsomes, (b) rat intestine microsomes, (c) human liver microsomes, and (d) human intestine microsomes, (2 mg/mL final concentration microsomal protein) after 15 min incubation at 37 °C and based on detection at 345 nm.

To identify the exact position of the glucuronosyl moiety in the luteolin conjugates, ^{1}H NMR analysis was performed. Table 2 presents the ^{1}H NMR chemical shift values and coupling constants of the reference compounds luteolin, luteolin-7-*O*-glucoside and luteolin-4′-*O*-glucoside. Identification of the various ^{1}H NMR resonances has been achieved on the basis of comparison to literature data (*32*) and of their splitting patterns. Table 2 also summarizes the ^{1}H NMR chemical shift values and coupling constants of the three metabolites with retention times at 11.4, 13.9, and 14.5 min. Comparison of the chemical shift values of the aromatic protons of the glucuronosyl adduct with retention time 11.4 min to the ^{1}H NMR resonances of luteolin reveals a change of +0.24 ppm and +0.35 ppm, respectively, in the chemical shift value of the NMR resonances of especially the C6−H and the C8−H with their $^4J_{HH}$ coupling of 2.1 Hz (Table 2). In contrast, the ^{1}H NMR signals of C2′-H, C5′-H, C6′-H, and C3−H are unaffected in the ^{1}H NMR spectrum of this glucuronosyl metabolite as compared to luteolin. In addition the ^{1}H NMR characteristics of this metabolite

Table 1. Percentages of Metabolites Formed from Luteolin and Quercetin with Microsomes from Different Sources Based on Peak Area Measured by HPLC at 345 nm for Luteolin and 370 nm for Quercetin[a]

Luteolin

microsomes	t_R 11.4 min 7-*O*-Gluc (%)	-	t_R 13.9 min 4′-*O*-Gluc (%)	t_R 14.5 min 3′-*O*-Gluc (%)	substrate conversion (%)
rat liver	28	-	11	61	21
rat intestine	32	-	3	65	27
human liver	77	-	6	17	27
human intestine	5	-	44	51	74

Quercetin

microsomes	t_R 10.5 min 7-*O*-Gluc (%)	t_R 10.7 min 3-*O*-Gluc (%)	t_R 13.7 min 4′-*O*-Gluc (%)	t_R 14.2 min 3′-*O*-Gluc (%)	substrate conversion (%)
rat liver	40	0	18	42	18
rat intestine	41	9	4	46	25
human liver	65	13	3	19	22
human intestine	4	20	27	49	61

[a] The final microsomal protein concentration was 0.5 mg/mL.

Table 2. ^{1}H NMR Chemical Shift Values and Coupling Constants of Luteolin and Some Conjugates Measured in DMSO-d_6[a]

	C_6-H	C_8-H	C_3-H	C_5'-H	C_2'-H	C_6'-H
luteolin	6.14 $J_{H6-H8} = 2.1$ Hz	6.40 $J_{H8-H6} = 2.1$ Hz	6.63	6.84 $J_{H5'-H6'} = 8.3$ Hz	7.35 $J_{H2'-H6'} = 2.1$ Hz	7.37 $J_{H6'-H2'} = 2.1$ Hz $J_{H6'-H5'} = 8.3$ Hz
luteolin-7-*O*-glucoside	6.44 (+0.30) $J_{H6-H8} = 2.1$ Hz	6.79 (+0.39) $J_{H8-H6} = 2.1$ Hz	6.76 (+0.13)	6.90 (+0.06) $J_{H5'-H6'} = 8.4$ Hz	7.42 (+0.07) $J_{H2'-H6'} = 2.1$ Hz	7.45 (+0.08) $J_{H6'-H2'} = 2.1$ Hz $J_{H6'-H5'} = 8.4$ Hz
luteolin-4′-*O*-glucoside	6.19 (+0.05) $J_{H6-H8} = 2.1$ Hz	6.49 (+0.09) $J_{H8-H6} = 2.1$ Hz	6.83 (+0.20)	7.23 (+0.39) $J_{H5'-H6'} = 8.5$ Hz	7.50 (+0.15) $J_{H2'-H6'} = 2.1$ Hz	7.52 (+0.15) $J_{H6'-H2'} = 2.1$ Hz $J_{H6'-H5'} = 8.5$ Hz
metabolite t_R 11.4 min	6.38 (+0.24) $J_{H6-H8} = 2.1$ Hz	6.75 (+0.35) $J_{H8-H6} = 2.1$ Hz	6.72 (+0.09)	6.85 (+0.01) $J_{H5'-H6'} = 8.4$ Hz	7.39 (+0.04) $J_{H2'-H6'} = 2.1$ Hz	7.41 (+0.04) $J_{H6'-H2'} = 2.1$ Hz $J_{H6'-H5'} = 8.4$ Hz
metabolite t_R 13.9 min	6.15 (+0.01) $J_{H6-H8} = 1.8$ Hz	6.45 (+0.05) $J_{H8-H6} = 1.8$ Hz	6.78 (+0.15)	7.21 (+0.37) $J_{H5'-H6'} = 8.9$ Hz	7.45 (+0.10) $J_{H2'-H6'} = 1.8$ Hz	7.49 (+0.12) $J_{H6'-H2'} = 1.8$ Hz $J_{H6'-H5'} = 8.9$ Hz
metabolite t_R 14.5 min	6.17 (+0.03)	6.81 (+0.41)	6.55 (−0.08)	6.96 (+0.12)	7.64 (+0.29)	7.80 (+0.43)

[a] The ppm shift of the protons in the conjugates compared to the same protons in luteolin are put into brackets. The ppm values of the two reference compounds, luteolin-7-glucoside and luteolin-4′-glucoside, were assigned based on comparison to literature data (*32*). ^{1}H NMR identification of the metabolite of luteolin with retention time of 14.5 min was somewhat hampered by its instability, preventing identification of all splitting patterns although major resonance chemical shift values could still be observed.

resemble those of the reference compound luteolin-7-glucoside. All together these ^{1}H NMR data identify the microsomal luteolin monoglucuronosyl metabolite with retention time of 11.4 min as the 7-*O*-glucuronosyl of luteolin.

Comparison of the ^{1}H NMR data obtained for the metabolite with retention time of 13.9 min on HPLC with the ^{1}H NMR spectrum of luteolin reveals that the C5′-H, represented by a doublet at 6.84 ppm with a $^3J_{HH}$ coupling of 8.3 Hz, shifts by +0.37 ppm toward 7.21 ppm for this monoglucuronidated luteolin metabolite (Table 2). The ^{1}H NMR signal of C2′-H, shifts by +0.10 ppm, and that of C6′−H by +0.12 ppm. The ^{1}H NMR resonance of C6−H and C8−H are almost similar to those of C6−H and C8−H of luteolin. Together with the LC-MS results, this reveals that the metabolite is a monoglucuronosyl intermediate which can be identified as luteolin-4′-*O*-glucuronosyl.

^{1}H NMR identification of the third mono-glucuronosyl metabolite of luteolin with retention time of 14.5 min was somewhat hampered by its instability preventing identification of all splitting patterns although major resonance chemical shift values could still be observed. On the basis of LC-MS analysis, the metabolite is a monoglucuronosyl of luteolin. Together with the identification of the other two metabolites as the 4′-*O*- and the 7-*O*-glucuronosyl of luteolin, this metabolite can be either the 5-*O*- or the 3′-*O*-glucuronosyl of luteolin. On the basis of the presence of the resonance of the 5-OH group in the ^{1}H NMR spectrum of this metabolite at 12.95 ppm (data not shown) being a ^{1}H NMR visible OH resonance because of lack of rapid exchange with solvent due to strong hydrogen bonding of the OH-hydrogen to the 4-keto moiety, the metabolite cannot be the 5-*O*-glucuronosyl of luteolin. This indicates that the metabolite can be identified as the 3′-*O*-glucuronosyl of luteolin. This conclusion is corroborated by the fact that the chemical shift changes observed for the aromatic proton signals of this metabolite as compared to luteolin itself reveal significant changes in especially the ^{1}H NMR signal of C2′−H (+0.29 ppm) and C6′−H (+0.43 ppm), whereas the chemical shift value of C6−H and C3−H remain unaffected. This is in line with the identification of the metabolite as the 3′-*O*-glucuronosyl of luteolin. The unexpected relatively large shift in the ppm value of C8−H (+0.41 ppm) must then be ascribed to an intramolecular interaction between this C8−H and the glucuronosyl moiety attached at C3′-OH.

Identification of Quercetin Glucuronosyls. Similar experiments were conducted with quercetin as the model compound. Figure 3, panels a and c, shows the HPLC chromatograms of incubations of rat and human

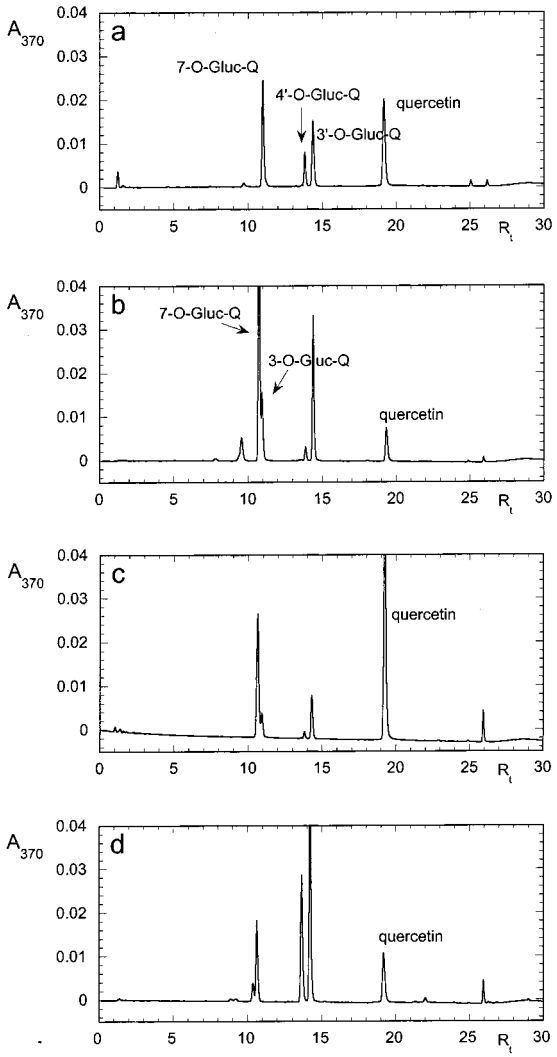

Figure 3. HPLC chromatogram of incubations of quercetin with (a) rat liver microsomes, (b) rat intestine microsomes, (c) human liver microsomes, and (d) human intestine microsomes (2 mg/mL final concentration microsomal protein) after 15 min incubation at 37 °C and based on detection at 370 nm.

liver microsomes with 100 μM quercetin in the presence of UDPGA. Figure 3, panels b and d, shows the HPLC chromatograms of similar incubations with rat and human intestine microsomes. The chromatograms reveal that, in contrast with luteolin, not three but four major metabolites, with retention times at 10.5 ± 0.2, 10.7 ± 0.2, 13.7 ± 0.2, and 14.2 ± 0.2 min, are formed in different ratios. Table 1 summarizes the ratios obtained in the different incubations. Comparison of these ratios reveals that also for quercetin, the regioselectivity of glucuronidation varies between organs and between species (Table 1). Increasing the concentration of microsomal protein in the incubations from 0.5 to 2 mg/mL increased the overall conversion upon 15 min incubation 2.5 times but did not affect the regioselectivity i.e., the ratio between the different conjugates formed.

Incubation of the samples with β-glucuronidase results in complete elimination of the metabolite peaks and a concomitant increase of the quercetin peak (HPLC chromatograms not shown), indicating that, as expected, all four metabolite peaks represent glucuronidated quercetin derivatives. To identify the exact nature of the glucuronosyl conjugates, samples from the microsomal incubations were also analyzed by LC-MS. The results obtained reveal for the four metabolites a *m/z* value of 477 representing the [M − H]-mass of a quercetin monoglucuronosyl.

Table 3 summarizes the ^{1}H NMR chemical shift values and coupling constants of three quercetin monoglucuronosyls eluting from HPLC with retention times 10.5, 13.7, and 14.2 min as well as of quercetin and the reference compounds quercetin-3-*O*-glucoside (isoquercetrin) and quercetin-4′-*O*-glucoside (spiraeoside).

Identification of the various ^{1}H NMR resonances has been achieved on the basis of chemical shift values and their splitting patterns and for the quercetin monoglucuronosyl metabolites also on the basis of comparison with the data of the reference compounds. Comparison of the resonances of the aromatic protons of the metabolite eluting from the HPLC at retention time 10.5 min to the resonances of quercetin shows a shift of +0.22 ppm for the C6−H signal and an even larger shift of +0.35 ppm for the C8−H chemical shift value. In contrast, the chemical shift values of the protons on the B-ring are almost unaffected (Table 3). This result identifies the major metabolite of the quercetin incubations with liver microsomes, with a retention time of 10.5 min, as the 7-*O*-glucuronosyl of quercetin.

The ^{1}H NMR resonances of the metabolite with retention time 13.7 min on HPLC are similar to those previously published for spiraeoside (4′-*O*-glucoside of quercetin) (*32*) and show a shift of +0.37 ppm for the C5′−H ^{1}H NMR signal as the only difference compared to the ^{1}H NMR data of quercetin. Together with the LC-MS results, these NMR data identify this metabolite as quercetin 4′-O-glucuronosyl.

Comparison of the ^{1}H NMR data obtained for the metabolite with a retention time of 14.2 min on HPLC with the ^{1}H NMR resonances of quercetin reveals a change of +0.37 and +0.31 ppm, respectively, in the chemical shift value of the NMR resonances of the C6′−H and C2′−H (Table 3), while the chemical shift value of the C5′−H shows only a small shift of +0.09 ppm. This metabolite can be ascribed to be the 3′-*O*-glucuronosyl of quercetin. This is further supported by the similarity of its UV-absorption spectrum to that of the metabolite identified as the 4′-*O*-glucuronosyl of quercetin, the fact that its retention time on HPLC is slightly larger than that of the 4′-*O*-glucuronosyl conjugate, an elution order as observed for the 3′-*O*- and the 4′-*O*-glucuronosyl conjugate of luteolin (Figure 2), and by the LC-MS results which reveal this metabolite to be a monoglucuronidated intermediate. These results identify this metabolite as quercetin-3′-*O*-glucuronosyl.

The metabolite with a retention time of 10.7 min on HPLC is present in the quercetin incubation with human intestine microsomes (Figure 3d), but is only a minor product in the rat intestine and human liver incubations (Figure 3, panels b and c) or is even absent in the rat liver incubations (Figure 3a). The chemical instability of this metabolite during freeze-drying and subsequent NMR measurement overnight hampered its further identification by ^{1}H NMR (*33*). Since the LC-MS data indicated it to be a monoglucuronosyl of quercetin, and the 7-*O*-, 3′-*O*-, and 4′-*O*-monoglucuronosyls were already identified, the one residual monoglucuronosyl can be the 3-*O*- or the 5-*O*-glucuronosyl of quercetin. It has been published (*34*) that the 5-position only reacts if this is the only hydroxyl available. Due to the strong hydrogen

Table 3. ^{1}H NMR Chemical Shift Values and Coupling Constants of Quercetin and Some Conjugates Measured in DMSO-d_6[a]

	C_6-H	C_8-H	C_5'-H	C_2'-H	C_6'-H
quercetin	6.18 $J_{H6-H8} = 2.1$ Hz	6.40 $J_{H8-H6} = 2.1$ Hz	6.87 $J_{H5'-H6'} = 8.5$ Hz	7.67 $J_{H2'-H6'} = 2.1$ Hz	7.53 $J_{H6'-H2'} = 2.1$ Hz $J_{H6'-H5'} = 8.5$ Hz
isoquercetrin (3-*O*-GlcQ)	6.20 (+0.02) $J_{H6-H8} = 2.1$ Hz	6.40 (+0) $J_{H8-H6} = 2.1$ Hz	6.84 (−0.03) $J_{H5'-H6'} = 8.9$ Hz	7.57 (−0.10)	7.58 (+0.05) $J_{H6'-H5'} = 8.9$ Hz
spiraeoside (4′-*O*-GlcQ)	6.22 (+0.04) $J_{H6-H8} = 2.0$ Hz	6.46 (+0.06) $J_{H8-H6} = 2.0$ Hz	7.26 (+0.39) $J_{H5'-H6'} = 8.7$ Hz	7.71 (+0.04) $J_{H2'-H6'} = 2.2$ Hz	7.63 (+0.10) $J_{H6'-H2'} = 2.2$ Hz $J_{H6'-H5'} = 8.7$ Hz
metabolite t_R 10.5 min	6.40 (+0.22) $J_{H6-H8} = 1.9$ Hz	6.75 (+0.35) $J_{H8-H6} = 1.9$ Hz	6.89 (+0.02) $J_{H5'-H6'} = 8.4$ Hz	7.70 (+0.03) $J_{H2'-H6'} = 1.9$ Hz	7.57 (+0.04) $J_{H6'-H2'} = 1.9$ Hz $J_{H6'-H5'} = 8.4$ Hz
metabolite t_R 13.7 min	6.18 (+0) $J_{H6-H8} = 1.9$ Hz	6.45 (+0.05) $J_{H8-H6} = 1.9$ Hz	7.24 (+0.37) $J_{H5'-H6'} = 8.7$ Hz	7.70 (+0.03) $J_{H2'-H6'} = 1.9$ Hz	7.60 (+0.07) $J_{H6'-H2'} = 1.9$ Hz $J_{H6'-H5'} = 8.7$ Hz
metabolite t_R 14.2 min	6.16 (−0.02)	6.59 (+0.19)	6.96 (+0.09) $J_{H5'-H6'} = 8.3$ Hz	7.98 (+0.31)	7.90 (+0.37) $J_{H6'-H5'} = 8.3$ Hz

[a] The ppm shift of the protons in the conjugates compared to the same protons in quercetin are put into brackets. The ppm values of spiraeoside were taken from literature and the ones of isoquercetrin assigned based on comparison to literature data (*32*). ^{1}H NMR identification of the metabolite of quercetin with retention time of 14.2 min was somewhat hampered by its instability, preventing identification of all splitting patterns although major resonance chemical shift values could still be observed.

bonding of the 5-OH-hydrogen with the 4-keto, conjugation of this 5-OH does not readily occur. This leaves the 3-position as the only remaining possibility for monoglucuronosyl conjugated quercetin metabolites. The UV-absorption spectrum of the metabolite at 10.7 min shows a relatively large shift of band I from 370 nm in quercetin to 354 nm. It is reported (*29*) that this relatively large shift of the hypsochromic Band I, with a value of 12−17 nm points at conjugation at the 3-hydroxyl of quercetin. Taking these considerations into account, it can be concluded that this metabolite with a retention time of 10.7 min on HPLC must be the 3-*O*-monoglucuronosyl of quercetin.

Conversion of Luteolin and Quercetin by Individual UDP-Glucuronosyltransferases. In a subsequent series of incubations, the model flavonoids of the present study were incubated with Supersomes containing specific individual UDP-glucuronosyltransferases. As an example, Figure 4 presents the HPLC chromatograms of incubations of UGT1A1, UGT1A6, and UGT1A9 with luteolin (Figure 4, panels a−c) and quercetin (Figure 4, panels d−f). These chromatograms represent the ones with the highest levels of metabolite formation or with different behavior between luteolin and quercetin conversion. Table 4 presents the relative percentages of substrate conversion in 30 min incubations as well as the regioselectivities observed for the incubations of luteolin and quercetin with UGT1A1, 1A3, 1A4, 1A6, 1A8, 1A9, 1A10, 2B7, and 2B15.

Major metabolites observed were similar to the ones observed in the microsomal incubations and identified as 3-*O*-glucuronosyl (only with quercetin), 7-*O*-, 3′-*O*-, and 4′-*O*-glucuronosyls of the respective flavonoid. The data reveal that these isoenzymes generally do not make a single glucuronosyl metabolite but rather make a mixture of 3-*O*-, 7-*O*-, 3′-*O*-, and 4′-*O*-glucuronosyls in varying ratios (Table 4). Also important to derive from these data is that preference of an isoenzyme for a specific site of glucuronidation with one flavonoid (for example, the 7-OH for luteolin by UGT1A3) does not necessarily imply preferential glucuronidation at the same position for a structurally related flavonoid, since UGT1A3 preferentially generates the 3′-*O*-glucuronosyl of quercetin. Another example of a striking discrepancy is the generation of all three glucuronosyls, i.e., 7-*O*-, 3′-*O*-, and 4′-*O*- from luteolin, but the highly preferential 3′-*O*-glucuronosyl formation for quercetin by UGT1A1 and UGT1A8 (Figure 4, panels a and d, Table 4). In addition, efficient conversion of one flavonoid apparently does not imply efficient conversion of the related compound, as illustrated by the fact that UGT1A6 hardly converts quercetin (Figure 4e), but forms significant levels of the 7-*O*-glucuronosyl from luteolin (Figure 4b).

Thus, the results obtained reveal that regioselectivity is dependent on the model flavonoid of interest and the UDP-glucuronosyltransferase involved, UGT1A1, UGT1A8, and UGT1A9 being especially active in flavonoid conjugation whereas the isoenzymes UGT1A4, UGT1A10, and the isoenzymes from the UGTB family, UGT2B7 and UGT2B15, are less efficient.

Discussion

In this study, the identification of phase II metabolites, resulting from glucuronidation of two flavonoid model compounds, i.e., luteolin and quercetin, was carried out using HPLC, LC/MS, and ^{1}H NMR. Incubation of luteolin and quercetin with rat as well as human liver microsomes resulted in the formation of 7-*O*-glucuronosyl and 3′-*O*-glucuronosyl conjugates of luteolin and -quercetin as major metabolites and the 4′-*O*-glucuronosyl derivative of both flavonoids as a third, but minor metabolite. In addition, quercetin, having a hydroxyl group at C3, was metabolized to its 3-*O*-glucuronosyl conjugate as well. Human and rat liver differ in the ratio of the metabolites produced. Using intestine microsomes from human and rat, it could be demonstrated that the type of metabolites formed are the same as those formed by liver microsomes, although regioselectivities of the glucuronidation vary significantly.

Several studies report glucuronidated quercetin metabolites in in vitro microsomal studies. Crespy et al. (*19*) reported four unidentified glucuronosyl type metabolites, when investigating the quercetin glucuronidating capacity of microsomes from jejunum and ileum of rats. Morand et al. (*18*) reported four glucuronosyls of quercetin upon incubation of rat liver and cecal microsomal fractions. Although LC-MS data are required to substan-

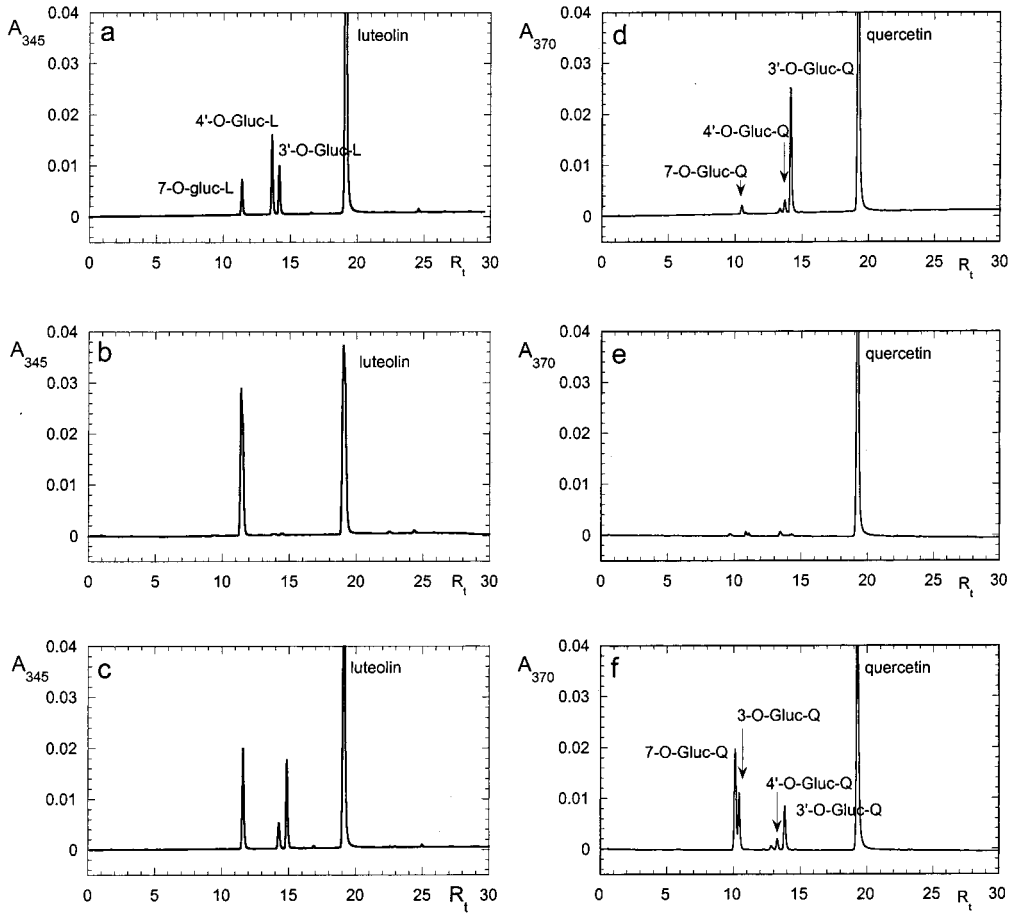

Figure 4. HPLC chromatogram of incubations of luteolin with (a) UGT1A1 (b) UGT1A6 and (c) UGT1A9 and of quercetin with (d) UGT1A1 (e) UGT1A6 and (f) UGT1A9 after 30 min incubation at 37 °C and based on detection at 345 nm for luteolin and 370 nm for quercetin.

Table 4. Percentages of Metabolites Formed from Luteolin and Quercetin with Individual UDP-Glucuronosyltransferases, Based on Peak Area Measured by HPLC at 345 nm for Luteolin and 370 nm for Quercetin

Luteolin

UGT	t_R 11.4 min 7-O-Gluc (%)	-	t_R 13.9 min 4′-*O*-Gluc (%)	t_R 14.5 min 3′-*O*-Gluc (%)	substrate conversion (%)
UGT1A1	21	-	50	29	26
UGT1A3	54	-	28	18	7
UGT1A4	40	-	38	22	0.5
UGT1A6	98	-	1	1	40
UGT1A8	39	-	22	39	25
UGT1A9	49	-	12	39	31
UGT1A10	64	-	24	12	11
UGT2B7	19	-	4	77	10
UGT2B15	88	-	6	6	4

Quercetin

UGT	t_R 10.5 min 7-*O*-Gluc (%)	t_R 10.7 min 3-*O*-Gluc (%)	t_R 13.7 min 4′-*O*-Gluc (%)	t_R 14.2 min 3′-*O*-Gluc (%)	substrate conversion (%)
UGT1A1	6	0	9	85	30
UGT1A3	21	16	11	52	21
UGT1A4	0	0	54	46	1
UGT1A6	30	16	32	22	3
UGT1A8	13	8	9	70	20
UGT1A9	50	26	5	19	36
UGT1A10	38	35	14	13	9
UGT2B7	12	41	3	44	19
UGT2B15	56	0	24	20	4

tiate the monoglucuronidated nature of these metabolites reported in the literature, it is likely that, based on the results of the present study, formation of 7-*O*-, 3′-*O*-, 4′-*O*-, and 3-*O*-monoglucuronosyl quercetin was also observed in these previous studies.

Comparison of the conversion percentages of both rat and human microsomes (Table 1), expressed per milligram of microsomal protein, reveals that the human intestine microsomes cause a more extensive metabolism of both luteolin and quercetin than the liver microsomes.

These results illustrate that nonhepatic organs such as the small intestine should not be underestimated with respect to their flavonoid metabolizing capacities (*22*). This result is in accordance with the findings of Morand et al. (*18*) who compared the quercetin metabolising capacity of rat liver and cecum microsomal fractions and calculated that the capacity of the cecal wall to produce glucuronosyl conjugates of quercetin is significantly greater than that of the liver.

Several studies on the metabolism of flavonoids by intestine models have been performed. Shimoi et al. (*12*) investigated the absorption of luteolin by rat everted small intestine. Luteolin was recovered in rat plasma as two metabolites, which were not identified in detail, but proved to be glucuronidated or sulfated forms of O-methylated conjugates. Only a small part of the compound remained unconjugated. Spencer et al. (*20*) perfused the jejunum and ileum from rats with quercetin and luteolin. Luteolin yielded six glucuronosyls which were not identified. In the present study three glucuronosyl conjugates of luteolin, the 7-*O*-, the 3′-*O*-, and the 4′-*O*-glucuronosyl luteolin, could be identified using intestine microsomes from rat and man. Possibly, the additional conjugates found by Spencer et al. (*20*) were mixed conjugates arising from the combined action of UDP-glucuronosyltransferases and catechol-*O*-methyltransferases, also known to be present in the intestine and active in flavonoid phase II type metabolism. Zhu et al. (*15*) even suggested that the rapid 3′-*O*-methylation of quercetin by catechol-*O*-methyl transferase found *in vivo* in hamsters could be an explanation for its lack of carcinogenicity in vivo.

Day et al. (*29*) reported formation of four glucuronosyl conjugates formed by incubation of quercetin with human liver microsomes. They determined the position of each quercetin glucuronosyl by using UV absorbance spectra and known shift reagents. In the present study, the glucuronosyl conjugates are identified with ^{1}H NMR, which is the method of choice for unambiguous identification. Similar sites for glucuronidation of quercetin were observed but the ratio of the formed products is different from that reported by Day et al. (*29*). In the present study, the 7-*O*-glucuronosyl is the major metabolite of the human liver incubation with quercetin, whereas Day et al. (*29*) have found that the 4′-OH is the preferential position for glucuronosyl conjugation. This difference in regioselectivity can be ascribed to a difference in the quercetin concentration used and the kinetic parameters ($v_{max\ app.}$ and K_m) for the different glucuronidations. Glucuronidation at the 7-OH having a high $v_{max\ app.}$ and a K_m of 6.5 μM, the 100 μM concentration of the present study as compared to 1 μM in the study of Day et al., explains the relatively high contribution of 7-*O*-glucuronidation in the present study.

The regioselectivity of glucuronosyl conjugation is not only dependent on the flavonoid of interest but also on the UDP-glucuronosyltransferase involved. Human UGT1A1, UGT1A8, and UGT1A9 were shown to be especially active in conjugation of both flavonoids whereas UGT1A4, UGT1A10, and the isoenzymes from the UGTB family, UGT2B7 and UGT2B15, were less efficient.

Qualitative comparison of the results obtained with human liver and intestine microsomal incubations and the regioselectivities found for the various human UGT isoenzymes may reveal to some extent which isoenzymes play an important role in the preferential site of glucuronosyl conjugation in the two tissues. The regioselectivity of luteolin and quercetin conjugation by human liver microsomes, correlates best with the pattern obtained with UGT1A9 and the human intestine incubations result in patterns of glucuronosyl conjugates, which match the UGT1A1 and UGT1A8 metabolite patterns best.

Cheng et al. (*35*) found that human UGT1A6 and UGT1A9 were not expressed in small intestine and colon, so not contributing to the first-line defense against phenolic xenobiotic compounds that are presented via the gut. They also reported that human UGT1A8 may be involved in flavonoid metabolism and displayed a higher glucuronidation rate than UGT1A10 toward these substrates. This is in line with the results obtained in the present study for UGT1A8 and UGT1A10 catalyzed conversion of quercetin and luteolin. Green et al. (*36*) found that UGT1A3 catalyzed the glucuronidation of flavonoids, e.g., quercetin. Results of the present study reveal that for luteolin and quercetin, the role of UGT1A9 (liver) and UGT1A1 and UGT1A8 (intestine) may be even more pronounced. King et al. (*37*) found that rat and human UGT1A1 exhibit comparable substrate specificity and efficiency of glucuronidation for flavonoids. In this study, it was found that the efficiency of glucuronidation of human UGT1A1 for luteolin and quercetin is indeed comparable, but that this UGT isoenzyme produces significant differences in the regioselectivity of glucuronidation for both flavonoids.

Finally, it is important to note that the position at which glucuronidation is occurring is of importance for the anti-oxidant as well as the pro-oxidant capacity of the flavonoids (*20*). Glucuronidation at the 7-*O*-position, is not thought to influence the anti-oxidant or pro-oxidant activity of the two flavonoids to a significant effect because this leaves the catechol moiety intact (*18*). Taking into account the fact that the anti-oxidant action (*18*, *20*, *38*) as well as the pro-oxidant toxicity (*10*) of these catechol-type flavonoids is especially related to their unconjugated 3′,4′-dihydroxyl moiety, it is of interest to note that the human intestine UGT(s) appear to be especially effective in conjugating this 3′,4′ catechol unit. This would imply that upon glucuronidation along the transport across the intestinal border the flavonoids loose a significant part of these biological activities.

Acknowledgment. This work was supported by the "NWO Stimuleringsprogramma Verantwoorde voeding" Project 014-12-012.

References

(1) Middleton, E., Jr., and Kandaswami, C. (1994) The impact of plant flavonoids on mammalian biology: implications for immunity, inflammation and cancer. In *The flavonoids: advances in research since 1986* (Harborne, J. B., Ed.) pp 619−652, Chapman & Hall, London.

(2) Rice-Evans, C. A., Miller, N. J., and Paganga, G. (1996) Structure-antioxidant activity relationships of flavonoids and phenolic acids. *Free Radical Biol. Med.* **20**, 933−956.

(3) Diplock, A. T., Charleux, J.-L., Crozier-Willi, G., Kok, F. J., Rice-Evans, C. A., Roberfroid, M., Stahl, W., and Vina-Ribes, J. (1998) Functional food science and defence against reactive oxygen species. *Br. J. Nutr.* **80** (Suppl. 1), S77−S112.

(4) Penning, T. M., Burczynski, M. E., Hung, K. D., McCoull, K. D., Palackal, N. T., and Tsuruda, L. S. (1999) Dihydrodiol dehydrogenases and polycyclic aromatic hydrocarbon activation: generation of reactive and redox active o-quinones. *Chem. Res. Toxicol.* **12**, 1−18.

(5) MacGregor, J. T., and Jurd, L. (1978) Mutagenicity of plant flavonoids: structural requirements for mutagenic activity in Salmonella typhymurium. *Mutat. Res.* **54**, 297−309.
(6) Mitchel, R. E. J., and McCann, R. (1993) Vitamin E is a complete tumor promotor in mouse skin. *Carcinogenesis* **14**, 659−662.
(7) Podmore, I. D., Griffiths, H. R., Herbert, K. E., Mistry, N., Mistry, P., and Lunec, J. (1998) Vitamin C exhibits pro-oxidant properties. *Nature* **392**, 559−559.
(8) Galati, G., Chan, T., Wu, B., and O'Brien, P. (1999) Glutathione-dependent generation of reactive oxygen species by the peroxidase-catalysed redox cycling of flavonoids. *Chem. Res. Toxicol.* **12**, 521−525.
(9) Bors, W., Heller, W., Michel, C., and Saran, M. (1990) Flavonoids as antioxidants: determination of radical-scavenging efficiencies. *Methods Enzymol.* **186**, 343−355.
(10) Boersma, M. G., Vervoort, J., Szymusiak, H., Lemanska, K., Tyrakowska, B., Cenas, N., Segura-Aguilar, J., and Rietjens, I. M. C. M. (2000) Regioselectivity and reversibility of the glutathione conjugation of quercetin quinone methide. *Chem. Res. Toxicol.* **13**, 185−191.
(11) Awad, H. M., Boersma, M. G., Vervoort, J., and Rietjens, I. M. C. M. (2000) Peroxidase-catalyzed formation of quercetin quinone methide-glutathione adducts. *Arch. Biochem. Biophys.* **378**, 224−233.
(12) Shimoi, K., Okada, H., Furugori, M., Goda, T., Takase, S., Suzuki, M., Hara, Y., Yamamoto, H., and Kinae, N. (1998) Intestinal absorption of luteolin and luteolin 7-O-*β*-glucoside in rats and humans. *FEBS Lett.* **438**, 220−224.
(13) Cao, G., Sofic, E., and Prior, R. L. (1997) Antioxidant and prooxidant behavior of flavonoids structure−activity relationships. *Free Radical Biol. Med.* **22**, 749−760.
(14) Brown, J. E., Khidr, H., Hider, R. C., and Rice-Evans, C. A. (1998) Structural dependence of flavonoid interactions with Cu^{2+} ions: implications for their antioxidant properties. *Biochem. J.* **330**, 1173−1178.
(15) Zhu, B. T., Ezell, E. L., and Liehr, J. G. (1994) Catechol-*O*-methyltransferase-catalyzed rapid O-methylation of mutagenic flavonoids. *J. Biol. Chem.* **269**, 292−299.
(16) Piskula, M. K., and Terao, J. (1998) Accumulation of (−)-epicatechin metabolites in rat plasma after oral administration and distribution of conjugation enzymes in rat tissues. *J. Nutr.* **128**, 1172−1178.
(17) Piskula, M. K., and Terao, J. (1998) Quercetin's solubility affects its accumulation in rat plasma after oral administration. *J. Agric. Food Chem.* **46**, 4313−4317.
(18) Morand, C., Crespy, V., Manach, C., Besson, C., Demigne, C., and Remesy, C. (1998) Plasma metabolites of quercetin and their antioxidant properties. *Am J. Physiol.* **275**, R212−R219.
(19) Crespy, V., Morand, C., Manach, C., Besson, C., Demigne, C., and Remesy, C. (1999) Part of quercetin absorbed in the small intestine is conjugated and further secreted in the intestinal lumen. *Am. J. Physiol.* **40**, G120−G126.
(20) Spencer, J. P., Chowrimootoo, G., Choudhury, R., Debnam, E. S., Srai, S. K., and Rice-Evans, C. (1999) The small intestine can both absorb and glucuronidate luminal flavonoids. *FEBS Lett* **458**, 224−230.
(21) Manach, C., Texier, O., Morand, C., Crespy, V., Tegerat, F., Demigne, C., and Remesy, C. (1999) Comparison of the bioavailability of quercetin and catechin in rats. *Free Radical Biol. Med.* **27**, 1259−1266.
(22) Williamson, G., Day, J., Plumb, G. W., and Couteau, D. (2000) Human metabolic pathways of dietary flavonoids and cinnamates. *Biochem. Soc. Transact.* **28**, 16−22.
(23) Hempel, J., Pforte, H., Raab, B., Engst, W., Bohm, H., and Jacobasch, G. (1999) Flavonols and flavones of parsley cell suspension culture change the antioxidative capacity of plasma in rats. *Nahrung* **43**, 201−204.
(24) Liu, C. S., Song, Y. S., Zhang, K. J., Ryu, J. C., Kim, M., and Zhou, T. H. (1995) Gas chromatographic/mass spectrometric profiling of luteolin and its metabolites in rat urine and bile. *J. Pharm. Biomed. Anal.* **13**, 1409−1414.
(25) Hertog, M. G. L., Hollman, P. C. H., Katan, M. B., and Kromhout, D. (1993) Intake of potentially anticarcinogenic flavonoids and their determinants in adults in The Netherlands. *Nutr. Cancer* **20**, 21−29.
(26) Manach, C., Texier, O., Regerat, F., Agullo, G., Demigne, C., and Remesy, C. (1996) Dietary quercetin is recovered in rat plasma as conjugated derivatives of isorhamnetin and quercetin. *Nutr. Biochem.* **7**, 375−380.
(27) Manach, C., Morand, C., Demigne, C., Texier, O., Regerat, F., and Remesy, C. (1997) Bioavailability of rutin and quercetin in rats. *FEBS Lett.* **409**, 12−16.
(28) Manach, C., Morand, C., Crespy, V., Demigne, C., Texier, O., Regerat, F., and Remesy, C. (1998) Quercetin is recovered in human plasma as conjugated derivatives which retain antioxidant properties. *FEBS Lett.* **426**, 331−336.
(29) Day, A. J., Bao, Y., Morgan, M. R. A., and Williamson, G. (2000) Conjugation position of quercetin glucuronides and effect on biological activity. *Free Radical Biol. Med.* **29**, 1234−1243.
(30) Rietjens, I. M. C. M., and Vervoort, J. (1989) Microsomal metabolism of fluoroanilines. *Xenobiotica* **19**, 1297−1305.
(31) Soffers, A. E. M. F., Ploemen, J. H. T. M., Moonen, M. J. H., Wobbes, T., van Ommen, B., Vervoort, J., van Bladeren, P. J., and Rietjens, I. M. C. M. (1996) Regioselectivity and quantitative structure activity relationships for the conjugation of a series of fluoronitrobenzenes by purified glutathione S-transferase enzymes from rat and man. *Chem. Res. Toxicol.* **9**, 638−646.
(32) Markham, K., Geiger, H. (1993) ^{1}H nuclear magnetic resonance spectroscopy of flavonoids and their glycosides in hexadeuterodimethylsulfoxide. In *The flavonoids: advances in research since 1986* (Harborne, J. B., Ed.) pp 441−497, Chapman and Hall, London.
(33) Wolfender, J.-L, Rodriguez, S., Hostettmann, K., and Hiller, W. (1997) Liquid chromatography/ultra violet/mass spectrometric and liquid chromatography/nuclear magnetic resonance spectroscopic analysis of crude extracts of gentianaceae species. *Phytochem. Anal.* **8**, 97−104.
(34) Boutin, J. A., Meunier, F., Lambert, P., Hennig, P., Bertin, D., Serkiz, B., and Volland, J. (1993) In vivo and in vitro glucuronidation of the flavonoid diosmetin in rats. *Drug Metab. Dispos.* **21**, 1157−1161.
(35) Cheng, Z. Q., Radominska Pandya, A., and Tephly, T. R. (1998) Cloning and expression of human UDP-glucuronosyltransferase (UGT) 1A8. *Arch. Biochem. Biophys.* **356**, 301−305.
(36) Green, M. D., King, C. D., Mojarrabi, B., Mackenzie, P. I., and Tephly, T. R. (1998) Glucuronidation of amines and other xenobiotics catalyzed by expressed human UDP-glucuronosyltransferase 1A3. *Drug Metab. Dispos.* **26**, 507−512.
(37) King, C. D., Green, M. D., Rios, G. R., Coffman, B. L., Owens, I. S., Bishop, W. P., and Tephly, T. R. (1996) The glucuronidation of exogenous and endogenous compounds by stably expressed rat and human UDP-glucuronosyltransferase 1.1. *Arch. Biochem. Biophys.* **332**, 92−100.
(38) van Acker, S. A. B. E., Plemper-van Balen, G., van den Berg, D.-J., Bast, A., and van der Vijgh, W. J. F. (1998) Influence of iron chelation on the antioxidant activity of flavonoids. *Biochem. Pharmacol.* **56**, 935−943.

TX0101705